Ru-Pt catalysts supported on Al2O3 and SiO2Al2O3 for the selective ring opening of naphthenes

María Vicerich, Viviana Benitez, María Sánchez, Catherine Especel, Florence Epron, Carlos Pieck

Ru-Pt CATALYSTS SUPPORTED ON Al_2O_3 AND SiO_2-Al_2O_3 FOR THE SELECTIVE RING OPENING OF NAPHTHENES

María A. Vicerich[1], Viviana M. Benitez[1], María A. Sánchez[1], Catherine Especel[2], Florence Epron[2], Carlos L. Pieck[1*]

[1] Instituto de Investigaciones en Catálisis y Petroquímica (INCAPE) (FIQ-UNL, CONICET), Santiago del Estero 2654, 3000 Santa Fe, Argentina.

[2] Université de Poitiers, CNRS UMR 7285, Institut de Chimie des Milieux et Matériaux de Poitiers (IC2MP), 4 rue Michel Brunet, TSA 51106, 86073 Poitiers Cedex 9, France.

*Author to whom correspondence should be addressed: pieck@fiq.unl.edu.ar

ABSTRACT

Alumina and silica-alumina supported Ru-Pt catalysts were evaluated for the ring opening of naphthenes. Pt, Ru and Ru-Pt catalysts were prepared by impregnation of inorganic precursors over γ-alumina and silica-alumina supports. The catalysts were evaluated by temperature programmed reduction (TPR), pyridine temperature programmed desorption (TPD), CO-FTIR and by test reactions of 33DM1B isomerization, cyclohexane dehydrogenation, cyclopentane hydrogenolysis and ring opening of decalin.

The strong interaction between the metals (Pt-Ru) was attributed to their reduction occurring simultaneously. The acidity and strength of the acid sites of the monometallic Ru catalyst were higher than those of the monometallic Pt catalyst. Total acidity (Lewis and Brønsted) and strength of the acid sites were higher for the silica-alumina supported catalysts. The silica-alumina catalysts had ten times more Brønsted acidity than the γ-alumina ones and an increased activity and selectivity to decalin ring opening products. Supported monometallic Ru had the best performance for the ring opening reaction.

KEYWORDS: Selective ring opening, decalin, Ru-Pt catalysts.

INTRODUCTION

Around 20% of the production of the units of fluid catalytic cracking corresponds to Light Cycle Oil (LCO) a by-product of low economic value. The LCO presents a low cetane number because it contains 80% aromatics, 70% with two rings.[1,2] For this reason, there is a high interest in improving the cetane number of LCO and hence its value as a fuel by selectively opening the naphthenic ring.[3]

Monofunctional acid (mainly different kinds of zeolites), monofunctional metallic and bifunctional catalysts have been proposed for performing the selective ring opening (SRO).[4–10]

Despite the great effort made by several research groups[9], the selective opening of naphthenic rings has not yet been applied industrially. This could be due to the low yields to ring opening (RO) products. Arve et al.[11] mentioned that the reported selectivities to RO products are generally lower than 30% at conversion levels above 90%. However conversion values up to 52% have been reported by Santi et al.[12] using a 3.5Ir/Rb,H-Beta catalyst. Another substantial disadvantage for its industrial application is the catalyst deactivation by coke deposition and sulfur poisoning.[11,13]

Although Ru has been widely reported about the ring opening of mono-naphthenic compounds due to its high hydrogenolytic activity, there are only a few works in the literature that report the opening of two-ring naphthenes using Ru catalysts. Kustov et al.[10] have reported that the addition of Pt to a Ru/SiO_2 catalyst decreases its activity and leads to an increase of the dehydrogenation reaction. Murzin et al. have curiously found that platinum was more active than ruthenium for the ring-opening of decalin. The selectivity to isomerization and ring opening products was higher for Ru-MCM-41 than for Pt-MCM-41.[14] Kumar et al.[15] have shown that the method of preparation of the catalyst greatly influences the activity and selectivity of zeolite supported Ru catalysts.

In this work Ru-based catalysts supported over a medium acidity support were tried in order to obtain an improved activity in ring opening of naphthenes, as probed by the test reaction of decalin. The catalysts were further characterized by other techniques and the catalytic results were rationalized on the basis of the measured properties and activity of the metal and acid functions.

MATERIALS AND METHODS

Catalyst preparation

Two supports of different acidity and high surface area were chosen, Al_2O_3 and SiO_2-Al_2O_3 (39.3 wt% of SiO_2 and 60.7 wt% of Al_2O_3). The alumina support was a γ-alumina (Ketjen CK-300) and the silica-alumina (with boehmite alumina phase) was Siral 40 from Sasol. The two supports were calcined in air at 500 °C for 4 h to remove traces of organic binders. Then they were impregnated at room temperature with the appropriate amount of a solution of the precursor salts (H_2PtCl_6 and $RuCl_3$). The samples were then dried to 70 °C to a dry powder and left to rest at 120 °C in a stove for 12 h. The catalysts were further calcined (air, 4 h, 300 °C) and reduced (H_2, 4 h, 500 °C). The monometallic catalysts had a final nominal content of 1 wt% of Pt or Ru. Bimetallic catalysts had 0.5 wt% Ru and 0.5 wt% Pt. The catalysts were named with reference to the composition of the metal phase (Ru, Pt, Ru-Pt) and the kind of support (Al, SiAl).

Determination of the Pt and Ru contents

The metal content of the catalysts after the activation treatment was determined by inductively coupled plasma-optical emission spectroscopy (ICP-OES). Catalyst samples were previously dissolved in an acid solution and diluted.

Specific Surface area (BET)

The specific surface area (BET method) was determined in an automatic Micromeritics ASAP-2020 equipment by means of nitrogen adsorption at -196 °C. Catalyst samples were previously degassed at 250 °C for 2 h.

Temperature programmed reduction (TPR)

A Micromeritics Autochem II equipment was used to assess the reducibility of the samples. For the assays 200 mg of catalysts were previously calcined in air for 1 h at 350 °C, cooled to room temperature in an air flow. The system was swept with an argon stream and then the cell was heated to 600 °C at 10 °C min^{-1} in a flowing mixture reducing gas mixture (5% H_2 in Ar) while measuring the consumption of H_2 with a thermal conductivity detector.

Temperature programmed desorption of pyridine (TPD)

Pyridine was first adsorbed over the samples by dipping 200 mg of the catalyst in vial with pyridine at room temperature for many hours. Then the non-adsorbed pyridine was eliminated by

evaporation under a hood at room temperature. The dry powder obtained was then placed in the TPD cell and the physisorbed pyridine was stripped at 110 °C for 1 h in nitrogen flow (40 cm^3 min^{-1}). Then the temperature was varied from 110 to 650 °C at 10 °C min^{-1}. The amount of desorbed pyridine was measured by connecting the reactor exhaust to a flame ionization detector. The total amount of adsorbed pyridine was determined by comparing the area of the TPD traces with the area produced by calibrated pyridine pulses (1-2 µl) injected to the empty reactor.[16]

Isomerization of 3,3-dimethyl-1-butene (33DM1B)

The reaction was carried out in an U shaped microreactor, under conditions described elsewhere [17]. The catalyst (100 mg) was reduced in situ with H_2 (60 cm^3 min^{-1}, 300 ºC, 1 h). The catalyst was then cooled down to reaction temperature in N_2 (30 cm^3 min^{-1}). The feed was then injected (20.9 kPa partial pressure of 33DM1B, 15.2 mmol h^{-1} flowrate) and the products were analyzed by on-line gas chromatography.

CO chemisorption

The catalyst was placed in the reactor and reduced in hydrogen flow (500 °C, 1 h, 60 cm^3 min^{-1}). Then N_2 was fed for 1 h to desorb the hydrogen (500 °C, 60 cm^3 min^{-1}). Then the cell was cooled down to room temperature and pulses of CO (3.5% CO in N_2) were fed to the reactor. Non-chemisorbed CO was transformed into CH_4 over a Ni/Kieselguhr catalyst and detected in a flame ionization detector connected on-line.

CO-FTIR spectroscopy

A Nicolet 5ZDX spectrometer was used to obtain FTIR spectra at room temperature of the pre-reduced and outgassed catalysts. Experimental conditions have been previously reported.[18]. Self-supported wafers were reduced (300 °C, H_2, 30 min) and degassed at 10^{-4} Pa at 300 °C for 30 min. The first spectrum was obtained and the samples were put into contact with 4 kPa of CO. Then it was outgassed to 10^{-4} Pa at 25 °C for 30 min and a new spectrum was taken. The absorbance of chemisorbed CO was calculated as the difference of both spectra.

Cyclohexane dehydrogenation

Samples of 50 mg were placed in a tubular reactor. Then they were reduced in a stream of hydrogen (60 cm^3 min^{-1}, 300 °C) for 1 h. Conditions were then adjusted (300, 320, 335 and 350 °C; hydrogen flowrate = 80 cm^3 min^{-1}, pressure = 0.1 MPa, cyclohexane flowrate = 1.61 cm^3 h^{-1}) and the reaction was started. Reaction products were analyzed on-line using a Thermo Scientific Trace 1300 chromatograph with a ZB-1 Phenomenex capillary column.

Cyclopentane hydrogenolysis

150 mg of the catalysts were first placed in the reactor and reduced before the reaction (H_2, 60 cm^3 min^{-1}, 1 h, 250 °C). Reaction conditions were set at 0.1 MPa pressure, 40 cm^3 min^{-1} hydrogen flow rate, 0.483 cm^3 min^{-1} cyclopentane flow rate and 250 °C reaction temperature. Reaction products were analyzed on-line in a Thermo Scientific Trace 1300 chromatograph using a ZB-1 Phenomenex capillary column.

Selective ring opening of decalin (SRO)

A stainless-steel autoclave reactor was operated in batch mode. Reaction conditions were: reaction temperature = 350 °C, stirring rate = 1360 rpm, pressure = 3 MPa, decalin volume = 25 cm^3, weight of catalyst = 1 g, reaction time = 6 h. A sample was taken at the end of the reaction and analyzed using a Shimadzu-GC 2014 chromatograph with a ZB-5 Phenomenex capillary column and a flame ionization detector.

RESULTS AND DISCUSSION

Table 1 shows the values of Ru and Pt content as determined by ICP-OES analysis, specific surface area as determined by nitrogen sorptometry and hydrogen consumption during TPR tests. Values are also included of metal dispersion as calculated by CO chemisorption.

The theoretical and experimental metal content values are very close and show that the loss of Ru by formation of volatile compounds was negligible. Catalysts supported on Siral 40 have more than two times the specific surface area of the alumina supported ones. Moreover, it can be noted that for each series the specific surface area was practically the same. On the other hand, the metal dispersion values calculated assuming a CO/M=1 stoichiometry are very similar, i.e. the metal

particle sizes of the catalysts are very similar. There is practically no influence of the support or the nature of the metal.

The TPR traces of the catalysts are plotted in Figure 1. The Pt monometallic catalyst was reduced at a higher temperature than Ru on both supports. This is in good agreement with a report by Suppino et al.[19]. The Ru/Al monometallic catalyst had two reduction peaks, the first around 90 °C and the second at 153 °C, while the Ru/SiAl catalyst had a reduction peak at about 100 °C with a shoulder at about 140 °C. Previous reports[20] seem to suggest that the first peak may be due to the reduction of chlorinated species of Ru, while the smaller second peak can be due to the reduction of Ru oxide.[21,22] Bimetallic catalysts show a well-defined peak in the RuO_x reduction zone and a smaller peak at higher temperatures. The smaller peak can be attributed to the reduction of Pt oxides isolated from Ru while the main non-splitted peak should be attributed to the simultaneous reduction of Pt and Ru species. The shift of the reduction peak of Ru and Pt depending on the support is a consequence of the development of different metal-support interactions. Different values of metal dispersion should however not be excluded because the larger metal particles with less interaction with the support can be reduced at a lower temperature than the small particles with stronger interaction with the support.

Table 1 shows that the theoretical hydrogen consumption considering that the starting oxidized species are PtO_2 and RuO_2 and that the final reduced species are metallic atoms coincides very well with the experimental values obtained by integration of the TPR traces (the maximum difference between theoretical and experimental values was lower than 7 %). Since the TPR traces have reached the base line level at 500 °C the metals should be in the zerovalent state in the reaction conditions.

The temperature programmed desorption of pyridine provides information about the total amount of the Brønsted and Lewis acid sites of the support and the distribution of the acid strength. This technique however does not allow to distinguish between Brønsted and Lewis acid sites. Figure 2 shows the TPD traces of the Al and SiAl catalysts. The desorption of pyridine occurs at a higher temperature on the SiAl catalysts than on the Al catalysts.

These results point out a higher strength of the acid sites of the catalysts supported on silica-alumina. Acidity values (µmol of pyridine m^{-2} and µmol of pyridine g^{-2}) are shown in Table 2. On both supports the Ru monometallic catalyst was more acid than the Pt monometallic catalyst. Table 2 clearly shows that catalysts supported on silica-alumina have stronger acid sites than the catalysts supported on alumina. The catalysts supported on alumina had virtually only weak acid sites desorbing at temperatures lower than 400 °C. The values of total acidity in units of µmol of pyridine by m^2 of catalyst surface area were higher for the alumina supported catalysts in comparison to the Siral 40 ones.

The concentration of the Brønsted acid sites is proportional to the values of conversion of 33DM1B.[23] This reaction produces 2,3-dimethyl-2-butene and 2,3-dimethyl-1-butene through a protonic mechanism with a secondary carbocation intermediate.[24] Other products, like methylpentenes, were not detected and this was expected because they are produced only at reaction temperatures higher than 300 °C.[25] It can be seen in Figure 3 that SiAl catalysts had 10 times more Brønsted acid sites than the alumina catalysts. In both series the bimetallic catalyst had more Brønsted acid sites than the corresponding monometallic catalyst.

The FTIR spectra of chemisorbed CO are shown in Figure 4. Only data corresponding to the 1850-2150 cm^{-1} wavenumber range are presented. CO adsorbed on monometallic Ru catalysts showed two bands at about 2142 and 2041 cm^{-1}, and a shoulder at 2080 cm^{-1}. The main absorption band (2038-2042 cm^{-1}) was attributed to the CO linearly adsorbed on Ru°.[26–28]
The positions of the bands at 2142 and 2080 cm^{-1} are very similar to those found for Ru tricarbonyl complexes ($Ru_2(CO)_6Cl_4$) with strong absorption bands at 2143-2128 and 2075-2069 cm^{-1} and a weak one at 2015- 2010 cm^{-1} [26]. Narita et al.[29] proposed that these bands may be due to CO adsorption on $Ru^{\delta+}$ chlorinated species. Monometallic Pt catalysts had a broad absorption band centered at about 2070 cm^{-1} that was attributed to the Pt°-CO bond. It is worth noting that the absorption band of the Pt/Al catalyst is not perfectly Gaussian and seems to be composed of several absorption bands. This can be explained by a heterogeneous size distribution of the Pt metal particles. Ménorval et al.[30] reported that the frequency of the $\nu_{C=O}$ vibration changes with the particle size. In the case of the bimetallic catalysts, either supported on alumina or silica-alumina, a broad absorption band centered around 2050 and 2065 cm^{-1} was found. There would seemingly

exist a higher surface enrichment of Pt in the Ru-Pt/Al catalyst than in the Ru-Pt/SiAl catalyst because the absorption band is closer to the position of the band of the Pt/Al catalyst.

As both reactions are catalyzed by the metal sites the dehydrogenation of cyclohexane and the hydrogenolysis of cyclopentane are reactions widely used for evaluating the metal function of the catalysts. Cyclohexane dehydrogenation is considered to be an "easy" or “non-demanding” reaction, i.e. it does not need a special ensemble of atoms, whereas the hydrogenolysis of cyclopentane is a demanding reaction.[31–34]

The reaction of cyclohexane dehydrogenation was evaluated at four different temperatures in order to determine the activation energy. The Arrhenius plots of the mono and bimetallic catalysts assuming a first order reaction are shown in Figure 5. All catalysts have straight lines and it can therefore be concluded that in the used temperature range there were no diffusive limitations and the assumption of first order kinetics was adequate.

Table 3 reports the values of conversion of cyclohexane at 300 °C and the activation energy of the reaction for both series of catalysts. As expected, Pt catalysts were more active than the Ru catalysts and the bimetallic catalysts had an intermediate behaviour. It is worth noting that bimetallic catalysts had a higher cyclohexane dehydrogenation activity and a higher activation energy than the average between Pt and Ru monometallic catalysts. This could be explained by the existence of a surface enrichment of Pt species. Miura et al.[35] reported a surface enrichment in Pt in the bimetallic Pt-Ru particles supported on alumina and silica, which was attributed to the lower heat of sublimation of Pt. The values of the activation energy found for the Pt catalysts are in line with the values reported in the literature.[36–38] The activation energy of the Ru catalysts was close to 38.5 Kj mol^{-1} as stated by Goenin et al.[39] for Ru/SiO_2 catalysts. However the activation energy of the Ru catalyst was half that reported by Peden and Goodman[40] for Ru crystals (75.3 kj mol^{-1}).

In contrast to the results found for the dehydrogenation of cyclohexane the results of hydrogenolysis of cyclopentane showed the presence of a strong deactivation (results not shown) as a function of time-on-stream, likely due to carbon deposition, cyclopentane being a precursor of coke species.[41] For this reason, only the values at 7 min reaction time are reported, when the surface of the catalysts is supposedly “clean”. Results in Table 3 indicate that monometallic Ru catalysts are more active than Pt monometallic catalysts.[42,43] The bimetallic catalysts had lower

activity (lower conversion) than the average value of the monometallic catalysts. These results confirm the surface enrichment of Pt.

Criteria laid out by Santikunaporn et al.[4] and Chandra Mouli et al.[44] were used to lump the reaction products of decalin. The lumps are: (i) cracking products (CP), (ii) products of ring opening (RO), (iii) products of ring contraction (RC), (iv) dehydrogenated products (DH).
Figure 6 and Table 4 displays values of conversion and yield to different products at 6 h reaction time at 350 °C, respectively. In order to analyze the results, it is useful to examine the reaction mechanisms proposed for decalin ring opening. A monomolecular mechanism was proposed by Arribas and Martínez[45] for the hydrocracking of methylnaphthalene on bifunctional Pt/USY catalysts. In this mechanism the aromatic rings of methylnaphthalene are hydrogenated on Pt sites, with subsequent migration to Brønsted acid sites where isomerization (contraction) of the saturated C_6 rings to C_5 rings and further ring opening would occur.[12] This reaction mechanisms do not take into account the metal hydrogenolytic activity. On the other hand, the bifunctional ring opening mechanism assumes that the acid-controlled ring contraction occurs first and that the ring opening follows, catalyzed by the metal sites with hydrogenolytic activity. These rings are then hydrogenated over the metal sites.[6,46] The optimum catalyst should have high acidity, mainly of the Brønsted type, and hydrogenolytic activity.

Figure 6 shows that the catalysts supported on silica-alumina are more active (higher conversion) than those supported on alumina. This is related to the higher amount and strength of Brønsted acid sites of the silica-alumina support (Figure 2 and 3). For both supports it appears that the monometallic Ru catalysts are more active than the monometallic Pt ones, but the difference in decalin conversion is more pronounced on alumina than on silica-alumina. This is due to the higher hydrogenolytic activity of Ru as compared to Pt (Table 3).
For the alumina support, the incorporation of Pt to the Ru catalyst decreases its hydrogenolytic activity and leads to a lower yield to ring opening products. For the catalysts supported on SiAl, the yield to RO products is practically the same as the yields of monometallic Ru and bimetallic Ru-Pt. This could be due to monometallic Ru and Pt catalysts having similar yield to RO products. The greater yield to ring opening (RO) and ring contraction (RC) products of the silica-alumina catalysts can be attributed to its higher acidity (mainly of the Brønsted type). As mentioned before

the acid function of the catalysts promotes ring contraction. Compounds with smaller rings are easier to open on the metal function.[4]

Higher yields to cracking products are predicted for the silica-alumina catalysts because the formation of cracking products occurs by a bifunctional metal-acid mechanism in which the rate-controlling step is acid catalyzed.[47]

The yield to dehydrogenated products on the bimetallic catalysts is less than one fifth of the average yield obtained with the monometallic catalysts. This is an unexpected result because the bimetallic catalysts had an intermediate cyclohexane dehydrogenation activity. Koussathana et al.[48] found that hydrogenation of benzene and naphthalene were structure insensitive reactions when occurring on monometallic catalysts. They found however that the activity for hydrogenation of naphthalene and biphenyl varied very differently on the bimetallic catalysts. This was attributed to electronic modification of the metal by the formation an alloy and/or strong interaction between the metals.

CONCLUSIONS

Ru-Pt catalysts supported on silica-alumina and alumina have strong Ru-Pt interaction due to a simultaneous reduction during treatment in hydrogen flow. The quantity and strength of the acid sites of the silica-alumina catalysts was higher than those of the alumina catalysts. Silica-alumina acid sites were mostly of the Brønsted type. The different acidity was the main reason for the greater activity and yield to decalin opening products displayed by the silica-alumina catalysts.

Ru supported on Siral 40 had five times more yield to the desired products (ring opening compounds) than the Ru/Al_2O_3 catalyst.

REFERENCES

[1] S. Rabl, D. Santi, A. Haas, M. Ferrari, V. Calemma, G. Bellussi, J. Weitkamp, *Microporous and Mesoporous Materials* **2011**, *146*, 190.

[2] B. H. Cooper, B. B. L. Donnis, *Applied Catalysis A: General* **1996**, *137*, 203.

[3] U. Nylén, L. Sassu, S. Melis, S. Järås, M. Boutonnet, *Applied Catalysis A: General* **2006**, *299*, 1.

[4] M. Santikunaporn, J. E. Herrera, S. Jongpatiwut, D. E. Resasco, W. E. Alvarez, E. L. Sughrue, *Journal of Catalysis* **2004**, *228*, 100.

[5] A. Haas, S. Rabl, M. Ferrari, V. Calemma, J. Weitkamp, *Applied Catalysis A: General* **2012**, *425–426*, 97.

[6] H. Du, C. F. Fairbridge, H. Yang, Z. Ring, *Applied Catalysis A: General* **2005**, *294*, 1.

[7] P. Samoila, M. Boutzeloit, C. Especel, F. Epron, P. Marécot, *Journal of Catalysis* **2010**, *276*, 237.

[8] R. Moraes, K. Thomas, S. Thomas, S. Van Donk, G. Grasso, J. P. Gilson, M. Houalla, *Journal of Catalysis* **2012**, *286*, 62.

[9] A. Galadima, O. Muraza, *Fuel* **2016**, *181*, 618.

[10] L. M. Kustov, E. D. Finashina, V. I. Avaev, B. G. Ershov, *Fuel Processing Technology* **2018**, *173*, 270.

[11] K. Arve, P. Mäki-Arvela, K. Eränen, M. Tiitta, T. Salmi, D. Y. Murzin, *Chemical Engineering Journal* **2014**, *238*, 3.

[12] D. Santi, T. Holl, V. Calemma, J. Weitkamp, *Applied Catalysis A: General* **2013**, *455*, 46.

[13] E. Blanco, L. Piccolo, D. Laurenti, L. di Felice, N. Catherin, C. Lorentz, C. Geantet, V. Calemma, *Applied Catalysis A: General* **2018**, *550*, 274.

[14] D. Kubička, T. Salmi, M. Tiitta, D. Y. Murzin, *Fuel* **2009**, *88*, 366.

[15] N. Kumar, D. Kubicka, A. L. Garay, P. Mäki-Arvela, T. Heikkilä, T. Salmi, D. Y. Murzin, *Topics in Catalysis* **2009**, *52*, 380.

[16] L.S. Carvalho, C.L. Pieck, M.C. Rangel, N.S. Fígoli, C.R. Vera, J.M. Parera, Applied Catalysis A: General **2004**, 269, 105.

[17] S. A. D'Ippolito, C. Especel, L. Vivier, F. Epron, C. L. Pieck, Applied Catalysis A: General **2014**, 469, 532.

[18] V. A. Mazzieri, C. L. Pieck, C. R. Vera, J. C. Yori, J. M. Grau, Applied Catalysis A: General, **2009**, 353, 93.

[19] R. S. Suppino, R. Landers, A. J. G. Cobo, *Applied Catalysis A: General* **2016**, *525*, 41.

[20] V. A. Mazzieri, F. Coloma-Pascual, A. Arcoya, P. C. L'Argentière, N. S. Fıgoli, *Applied Surface Science* **2003**, *210*, 222.

[21] M. . Mendes, O. A. . Santos, E. Jordão, A. . Silva, *Applied Catalysis A: General* **2001**, *217*, 253.

[22] K. Y. Cheah, T. S. Tang, F. Mizukami, S. Niwa, M. Toba, Y. M. Choo, *Journal of the American Oil Chemists' Society* **1992**, *69*, 410.

[23] C. S. John, C. Kemball, R. A. Rajadhyaksha, *Journal of Catalysis* **1979**, *57*, 264.

[24] J. L. Lemberton, G. Perot, M. Guisnet, *Journal of Catalysis* **1984**, *89*, 69.

[25] E. A. Irvine, C. S. John, C. Kemball, A. J. Pearman, M. A. Day, R. J. Sampson, *Journal of Catalysis* **1980**, *61*, 326.

[26] S. Y. Chin, C. T. Williams, M. D. Amiridis, *The Journal of Physical Chemistry B* **2006**, *110*, 871.

[27] F. M. Hoffmann, M. D. Weisel, *Surface Science* **1992**, *269–270*, 495.

[28] W. K. Kuhn, J. He, D. W. Goodman, *Journal of Vacuum Science & Technology A: Vacuum, Surfaces, and Films* **1992**, *10*, 2477.

[29] T. Narita, H. Miura, K. Sugiyama, T. Matsuda, R. D. Gonzalez, *Journal of Catalysis* **1987**, *103*, 492.

[30] L.-C. de Ménorval, A. Chaqroune, B. Coq, and François Figueras, *Journal of the Chemical Society, Faraday Transactions* **1997**, *93*, 3715.

[31] J. A. Cusumano, G. W. Dembinski, J. H. Sinfelt, *Journal of Catalysis* **1966**, *5*, 471.

[32] D. W. Blakely, G. A. Somorjai, *Journal of Catalysis* **1976**, *42*, 181.

[33] C. Betizeau, G. Leclercq, R. Maurel, C. Bolivar, H. Charcosset, R. Frety, L. Tournayan, *Journal of Catalysis* **1976**, *45*, 179.

[34] M. Boudart, A. Aldag, J. E. Benson, N. A. Dougharty, C. Girvin Harkins, *Journal of Catalysis* **1966**, *6*, 92.

[35] H. Miura, T. Suzuki, Y. Ushikubo, K. Sugiyama, T. Matsuda, R. D. Gonzalez, *Journal of Catalysis* **1984**, *85*, 331.

[36] A. A. Susu, F. E. Enoh, A. F. Ogunye, *Journal of Chemical Technology and Biotechnology* **2007**, *30*, 735.

[37] L. I. Ali, A.-G. A. Ali, S. M. Aboul-Fotouh, A. K. Aboul-Gheit, *Applied Catalysis A: General* **1999**, *177*, 99.

[38] L. . Carvalho, C. L. Pieck, M. . Rangel, N. . Fígoli, J. . Grau, P. Reyes, J. M. Parera, *Applied Catalysis A: General* **2004**, *269*, 91.

[39] F. B. Goneim, A. A. Balandin, T. A. Slovokhotova, *Bulletin of the Academy of Sciences, USSR Division of Chemical Science* **1963**, *12*, 1758.

[40] C. H. F. Peden, D. W. Goodman, *Journal of Catalysis* **1987**, *104*, 347.

[41] C. L. Pieck, P. Marecot, J. M. Parera, J. Barbier, *Applied Catalysis A: General* **1995**, *126*,

153.

[42] C. G. Walter, B. Coq, F. Figueras, M. Boulet, *Applied Catalysis A: General* **1995**, *133*, 95.

[43] G. B. McVicker, M. Daage, M. S. Touvelle, C. W. Hudson, D. P. Klein, W. C. Baird, B. R. Cook, J. G. Chen, S. Hantzer, D. E. W. Vaughan, E. S. Ellis, O. C. Feeley, *Journal of Catalysis* **2002**, *210*, 137.

[44] K. C. Mouli, V. Sundaramurthy, A. K. Dalai, *Journal of Molecular Catalysis A: Chemical* **2009**, *304*, 77.

[45] M. A. Arribas, A. Martínez, *Applied Catalysis A: General* **2002**, *230*, 203.

[46] R. Moraes, K. Thomas, S. Thomas, S. Van Donk, G. Grasso, J. P. Gilson, M. Houalla, *Journal of Catalysis* **2013**, *299*, 30.

[47] A. Corma, V. González-Alfaro, A. V. Orchillés, *Journal of Catalysis* **2001**, *200*, 34.

[48] M. Koussathana, D. Vamvouka, H. Economou, X. Verykios, *Applied Catalysis* **1991**, *77*, 283.

Table 1. Metal content, specific surface area (BET), metal dispersion and hydrogen consumption.

Catalyst	Pt (wt%)	Ru (wt%)	S_{BET} [a] ($m^2\ g^{-1}$)	Metal Dispersion (%)	H_2 consumption (μmol $H_2\ g_{cat}^{-1}$) Theoretical	Experimental [b]
Ru/SiAl	-	0.92	422	51	182	184
Ru-Pt/SiAl	0.51	0.48	447	44	147	156
Pt/SiAl	0.98	-	456	53	100	105
Ru/Al	-	0.89	179	42	176	177
Ru-Pt/Al	0.49	0.42	182	50	133	138
Pt/Al	0.95	-	178	56	97	94

[a] S_{BET}: specific surface area. [b] H_2 consumption calculated from the area of the TPR trace.

Table 2. Total acidity of the catalysts determined by TPD of pyridine.

Catalyst	**Total acidity**		**Distribution of acid strength (μmol g^{-1})**		
	(μmol Py m^{-2})	**(μmol Py g^{-1})**	**T < 400 °C**	**400 °C < T < 500°C**	**T>500 °C**
Ru/SiAl	3.09	1303	208.5	924.9	169.6
Ru-Pt/SiAl	2.77	1238	312.6	703.9	221.5
Pt/SiAl	1.89	860	143.3	560.3	156.4
Ru/Al	3.49	625	469.0	130.0	26.0
Ru-Pt/Al	3.15	573	507.9	65.1	0.0
Pt/Al	2.71	482	364.8	104.2	13.0

Table 3. Values of conversion of cyclohexane (CH) at 300 °C and cyclopentane (CP) at 250 °C. Activation energy of the cyclohexane dehydrogenation reaction.

Catalyst	**Cyclohexane**		**Cyclopentane**
	Conversion (%)	**E_A (Kj mol^{-1})**	**Conversion (%)**
Ru/SiAl	24.2	28.5	58.0
Ru-Pt/SiAl	44.5	66.5	13.5
Pt/SiAl	49.7	95.0	11.4
Ru/Al	18.2	33.9	36.4
Ru-Pt/Al	52.8	65.7	18.4
Pt/Al	56.2	87.9	15.3
Mathematical average of monometallic catalyst of each series			
Ru-Pt/SiAl	36.95	61.9	34.70
Ru-Pt/Al	37.20	60.7	25.85

E_A: Activation energy of the CH dehydrogenation reaction.

Table 4. Decalin reaction results. Yields to different reaction products.

Catalysts	**RO**	**CP**	**RC**	**DH**
Ru/SiAl	16.88	2.60	2.50	1.92
Ru-Pt/SiAl	16.44	0.84	1.54	0.28
Pt/SiAl	14.42	0.96	2.05	2.67
Ru/Al	3.39	1.56	1.26	2.09
Ru-Pt/Al	1.82	1.06	0.40	0.52
Pt/Al	0.70	0.87	0.59	0.94

RO: ring opening products; CP: cracking products; RC: ring contraction products; DH: dehydrogenation products.

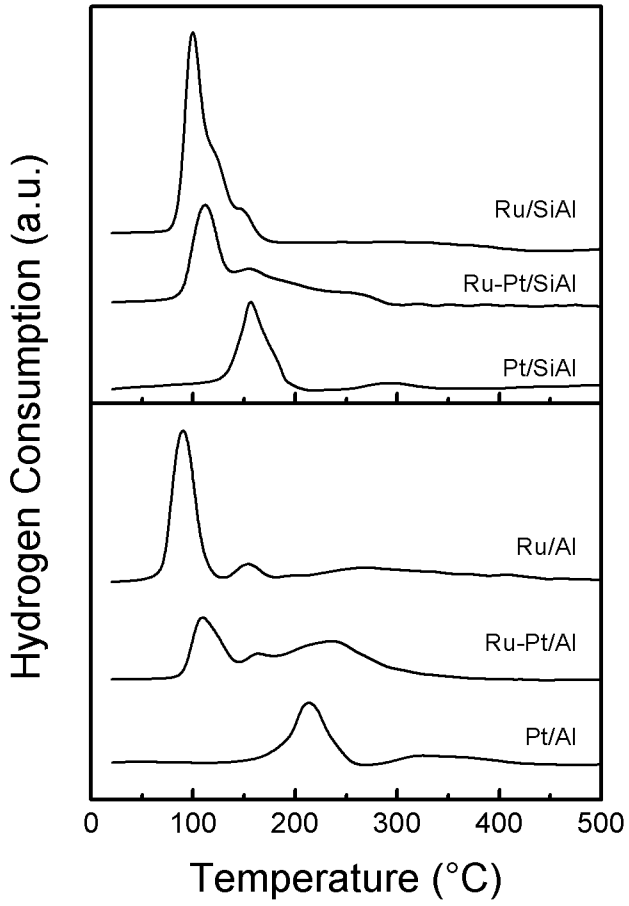

Figure 1. TPR results.

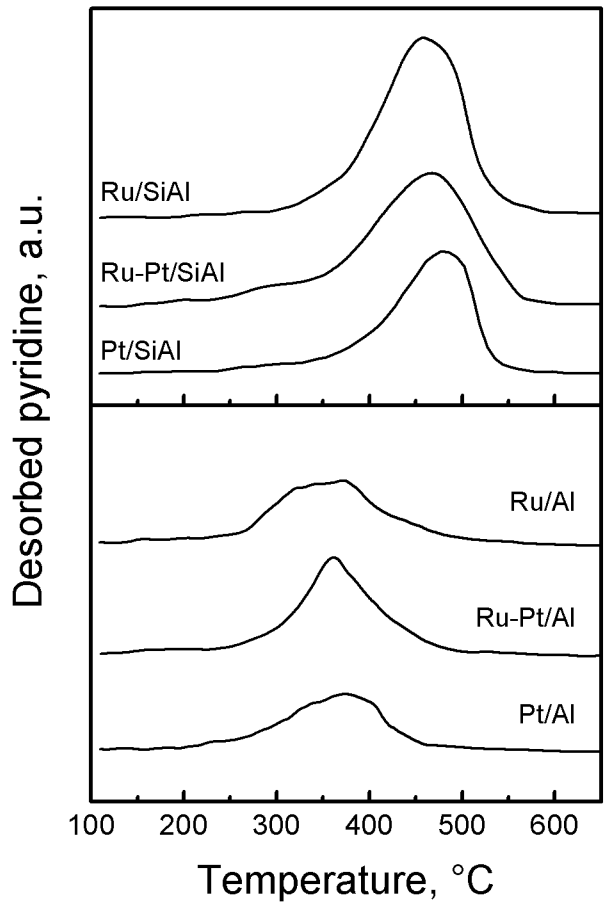

Figure 2. Pyridine TPD results.

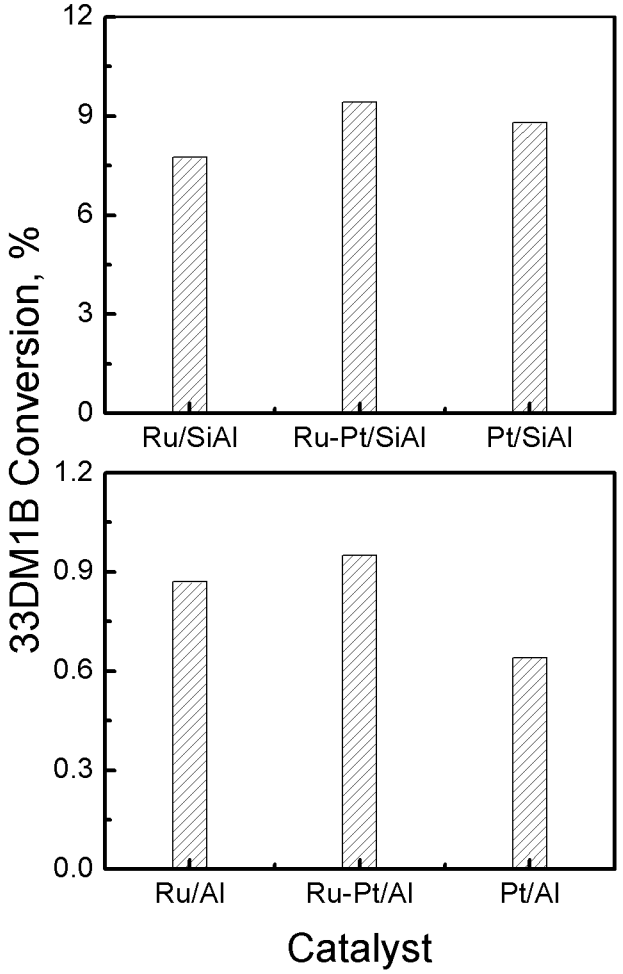

Figure 3. Brønsted acidity as determined from values of conversion of 33DM1B.

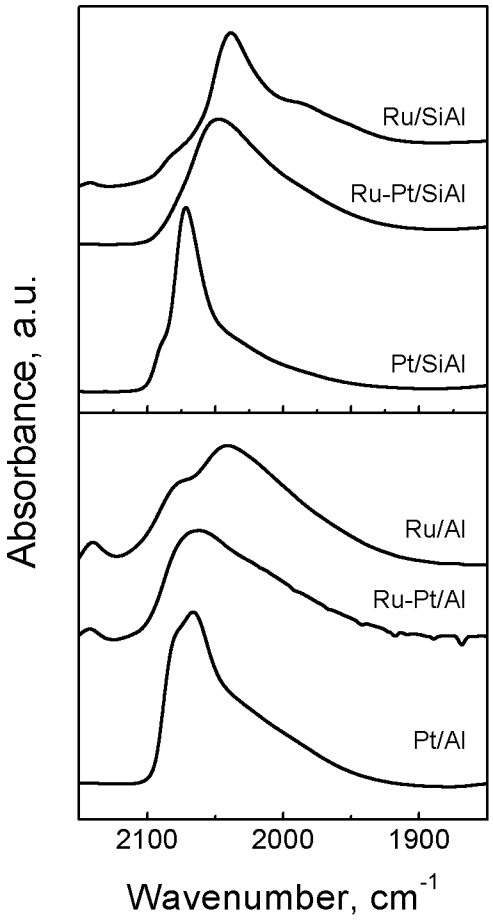

Figure 4. FTIR-CO absorption spectra.

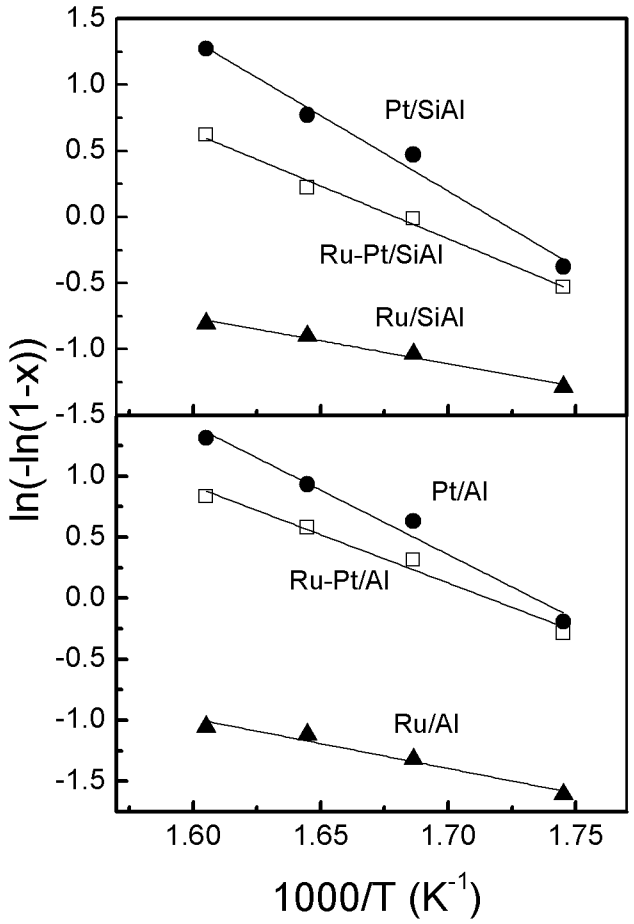

Figure 5. Arrhenius plots of the first order cyclohexane dehydrogenation.

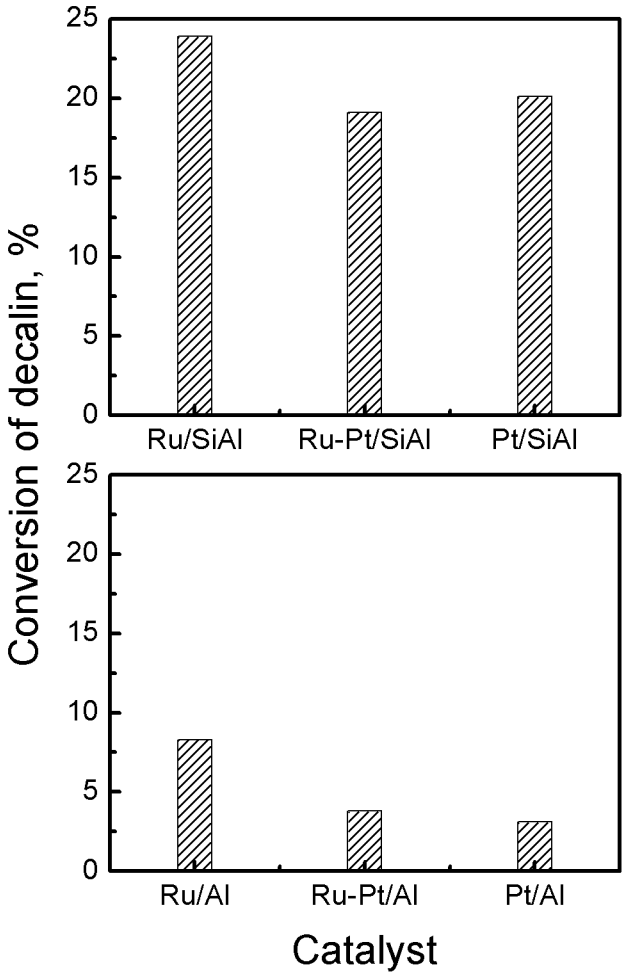

Figure 6. Conversion of decalin at 6 h reaction time and 350 °C.